
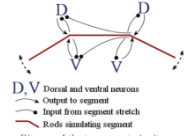
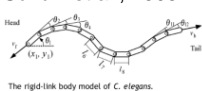
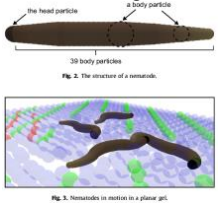
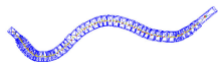

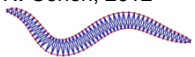


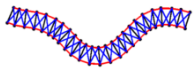
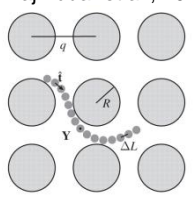
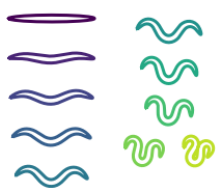
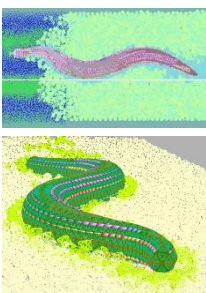
Tree-dimensional simulation of the *C. elegans* body and muscle cells in liquid and gel environments for behavioral analysis.

A. Palyanov, S. Khayrulin, S. D. Larson.

Supplemental Materials

1. Review of existing *C. elegans* locomotion and muscle/body models

Title / illustration	worm body complexity (resolution)	environment complexity and variety	biologically grounded	2D / 3D	direct muscle mapping	swimming/ crawling/ etc	free/ opensource/ other
Niebur and Erdős (1993) 	40 particles (19 segments)	simple		2D	no	crawling only	not known
Bryden and Cohen, 2004 	11 segments, each segment is represented by a single angle variable	simple		2D	no	crawling only	not known
Suzuki et al., 2005 	13 rigid links with 12 joints	simple, the environmental forces are not modelled		2D	no	crawling only	not known
Karbowski et al. 2008	12 sections, local flex angles	simple		2D	no	crawling only	ModelDB database
Rönkkö, Wong, 2008 	39 particles (partially overlapping spheres), each with its own radius, representing a worm body, connected with joints	planar gel / liquid tank / soil cube. No SPH or analog, gel/liquid/soil differ only in geometry, damping coefficient and gravity	There are 'liquid' particles, but no actual swimming observed or described in the paper	3D	no	"swimming" (movement through liquid particles), crawling	closed source
Mailler et al., 2010 	100 particles (25 discrete 3D box segments, geometry taken from photographs of living worms)	'agarose surface'	"The model is cross validated using video recording of worms during forward crawling"	3D	yes	crawling only	based on Open Dynamics Engine (ODE), which interfaces with JME using JME Physics
Palyanov et al., 2011 	~200 particles	'agar'	Body profile is reproduced along with all body wall muscle cells layout	3D	yes	Crawling only	Open Source
J.H. Boyle, S. Berry and N. Cohen, 2012 	98 particles (49 solid rods + a number of elastic connections)	'agar'	quite high	2D	yes, with 2D restrictions	crawling only	source code available

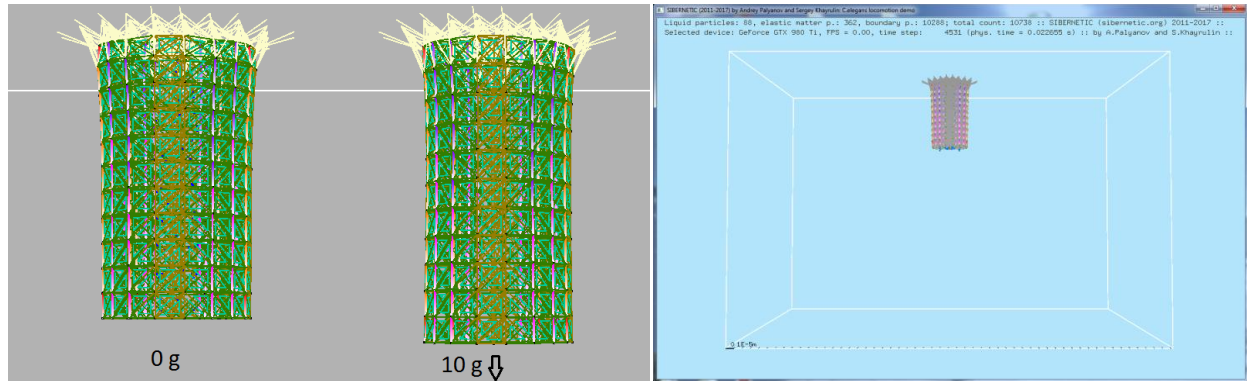
<p>Williamson 2012</p> 	<p>The worm is represented by 25 solid rods (50 discrete points) that give the worm its width, whose end points are connected laterally by damped springs representing the body wall muscles and diagonally by damped springs that serve to maintain the worm's internal pressure.</p>	<p>'agar'</p>	<p>"It should be noted that this model is not identical to that given in Boyle et al. (2012), but is based on a simpler version given in his PhD"</p>	<p>2D</p>	<p>yes, with 2D restrictions</p>	<p>crawling only</p>	<p>not mentioned in the paper, not found</p>
<p>Majmudar et al., 2012</p> 	<p>A mechanical worm (MW) model from a chain of elastically linked beads whose undulations are driven by a wave of torques along its length. The MW model incorporates contact interactions with the obstacles and goes beyond simple drag-based approximations of the hydrodynamic forces.</p>	<p>Liquid with obstacles</p>	<p>Capturing the swimmer-obstacle hydrodynamic interactions by solving the Stokes equations numerically and obtaining the flow field generated by the undulations and the constraints imposed by the obstacles.</p>	<p>2D</p>	<p>no</p>	<p>swimming only</p>	<p>not mentioned in the paper, not found</p>
<p>Fiesler, Kunert-Graf, Kutz (2017)</p>	<p>2D, 12 segments divided into 3 sub-segments, proprioception</p>	<p>'Water' & 'agar', same scheme as Boyle, Berri, Cohen</p>		<p>2D</p>	<p>yes</p>	<p>Crawling only</p>	<p>Open source</p>
<p>Cohen & Ranner (2017)</p> 	<p>No particles, finite element method. A continuum model of <i>C. elegans</i> biomechanics. Strictly inextensible body.</p>	<p>The model replicates behaviours across a wide range of environments A new numerical method that allows for simulations of arbitrary locomotion gait.</p>	<p>quite high</p>	<p>2D & 3D</p>	<p>a smooth and uniform muscle configuration along the body</p>	<p>Simulation results are reported only for crawling</p>	<p>For the numerical experiments presented in the paper the software package UMFPACK (Davis,2004) was used.</p>
<p>Palyanov et al., 2018 (Sibernetic)</p> 	<p>10143 elastic matter and 11436 liquid particles composing the worm body + hundreds of thousands particles representing the environment. 2290 elastic matter and 388 liquid particles composing worm body for half-resolution model.</p>	<p>Liquid, 'agar', elastic matter, static solid objects, any complex 3D combinations of them</p>	<p>high</p>	<p>3D</p>	<p>yes</p>	<p>swimming and crawling, reversal, omega-turn, body shortening</p>	<p>Open source</p>

Suppl. Table 1. Comparison with additional approaches to *C. elegans* modeling. Comparison between existing approaches to *C. elegans* modelling. As surveyed in the work of (Boyle et al., 2009 - *C. elegans* locomotion, an integrated approach) and taking into account other sources, up to date there are at least the following models of *C. elegans* locomotion mechanism.

The early models were two-dimensional and based on small number of either beads and joints (Bryden and Cohen, 2004; Suzuki et al., 2005) or 4-particle rectangular segments (Niebur, Erdős, 1993). Further (Ronkko and Wang, 2008) presented the first 3D model of worm body, represented as a sequence of 3D spherical beads of different diameters corresponding to worm body width profile along the direction from head to tail. Soon after that 3D models based on stacks (sequences) of squares (Mailler et al., 2010) and octagons (Palyanov et al., 2011) of a various sizes (to reproduce worm's width profile) connected by springs with each other.

2. Supplemental Methods

2.1. Muscle tests & strength calculations



Suppl. Figure 1. The scene used to measure the Young's modulus of the worm body (right) and a zoomed up view of the cross-section, used to determine the relationship of the strength of the muscles to the contraction speed of a cross-section of the body¹(left).

Our chosen values for single muscle force are within an interval between $-2 \cdot 10^{-3}$ to $+6 \cdot 10^{-3}$ μN (Fig 3B, right). Our comparison model for simulated muscle activity (Fig 3B, left; Boyle, Berri & Cohen, 2012), used single muscle force values between -8 to $+10$ μN , for a 100-fold difference in scale.

Previous experimental studies (Johari et al., 2013) measured the force generated by *C. elegans* as a whole rather than for a single muscle cell, and found values within 8-18 μN . This is on the same order as in Boyle et al., 2012, but in their case it is used for a single muscle cell. One explanation for the difference of more than 100 in the scales of the forces could be the presence of ~ 100 body wall muscles in *C. elegans* vs a single muscle cell.

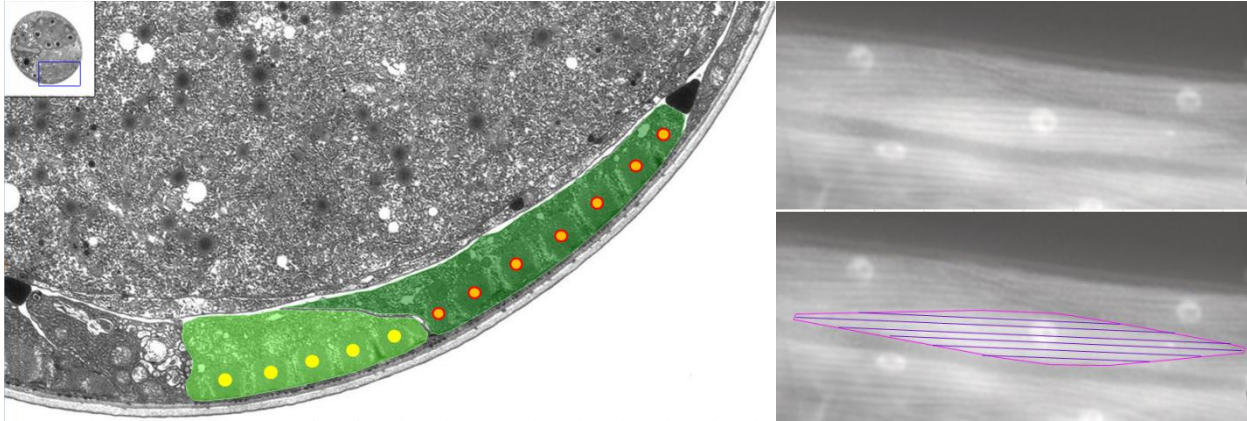
We used the following reasoning process to infer the value for maximal single muscle force. Our estimation is based on experimental data about the strength of a single muscle fiber (filament) multiplied by the number of such fibers in a typical *C. elegans* body wall muscle cell. A single muscle fiber generates force per cross-bridge within $(0.2-0.8) \cdot 10^{-6}$ μN according to (VanBuren et al., 1995)². In addition, the average length of a *C. elegans* muscle is about 80 μm , and thick filaments are 10 μm ³, so a full band is at least 20 μm , and a muscle fits about 2-3 bands separated by cross-bridges. Muscles have a rhomboid shape rather than a rectangular shape, so only the middle cross-section will have 7-8 A-bands (number of stripes in Suppl. Figure 2, right). Only the middle longitudinal cross-section will be composed of 4 cross-bridge bands, others will be shorter. Consequently, we estimated the number of muscle fibers in a *C. elegans* body wall muscle cell to be ~ 9300 ⁴. As a result, we estimate the force produced by a single muscle cell is equal to $((0.2-0.8) \cdot 10^{-6} \mu\text{N}) \cdot (500 \text{ filaments per A-band}) \cdot (7-8 \text{ A-bands in cross-section}) \cdot (2-3 \text{ cross-bridge bands in longitudinal cross-section}) = (1.4-9.6) \cdot 10^{-3} \mu\text{N}$, which is within the range of the Y-axis in Fig 3B.

¹ <https://www.youtube.com/watch?v=ayDprLG25IM>

² According to VanBuren et al., 1995, "In a direct comparison between smooth and skeletal muscle myosin, the average force per cross-bridge was 0.8 and 0.2 pN, respectively."

³ MusTable 2 from <http://www.wormatlas.org/ver1/handbook/mesodermal.htm/musclepartII.htm>

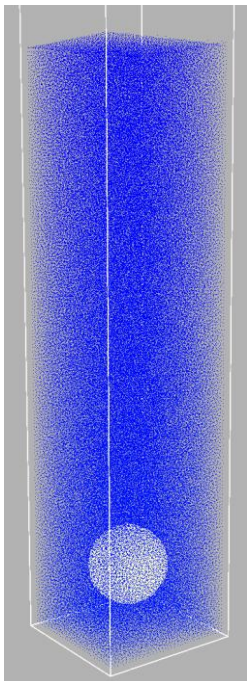
⁴ This is based on the microphotograph from SlidableWorm cross-section #273 in the middle of the worm body and MusFig37 from <http://www.wormatlas.org/ver1/handbook/mesodermal.htm/musclepartIII.htm> (one A-band of the muscle contains about 500 fibers, and a muscle in the middle of the body contains about 7-8 A-bands)



Suppl. Figure 2. On the left, A-bands in cross section in two muscles (yellow and orange). On the right, A-bands viewed in longitudinal cross section. Each pair of two adjacent purple lines outline an A-band. (Reproduced from WormAtlas with permission by Zeynep F. Altun).

The value chosen for the maximal force of a single muscle cell is consistent with a biophysical estimation from whole worm to single muscle, and from muscle fiber up to single muscle, and in addition it works well in concert with other simulation parameters.

2.2. Calculation of Viscosity in Sibernetic



We've suggested a way to measure viscosity in Sibernetic simulation - using Stokes's law: If the particle is falling in the viscous fluid under its own weight, then a terminal velocity, or settling velocity, is reached when this frictional force combined with the buoyant force exactly balances the gravitational force. This velocity, v (m/s), is given by:

$$v = \frac{2}{9} \cdot \frac{(\rho_p - \rho_f)}{\mu} \cdot gR^2$$

(vertically downwards if $\rho_p > \rho_f$, upwards if $\rho_p < \rho_f$), where:

- g is the gravitational acceleration (m/s^2) $g = 9.8 \text{ m/s}^2$ was used
- R is the radius of the spherical particle (m) $R = 0.05 \text{ mm}$ was used
- ρ_p is the mass density of the particles (kg/m^3) $\rho_p = 2000 \text{ kg/m}^3$ was used
- ρ_f is the mass density of the fluid (kg/m^3) $\rho_f = 1000 \text{ kg/m}^3$ was used
- μ is the dynamic viscosity ($\text{kg/m}\cdot\text{s}$) $\mu \approx 1.43 \text{ mPa}\cdot\text{s}$ was obtained

We have measured the terminal velocity in Sibernetic simulation and got the value $v = 0.015 \text{ m/s}$ (see Suppl. Figure 3). All the parameters of the liquid, as well as the scene scale, were the same which were used when simulating swimming *C. elegans*. Obtained result, $\mu = 1.43 \text{ mPa}\cdot\text{s}$, is very close to the case A ($1 \text{ mPa}\cdot\text{s}$) on the Fig. 2A from the paper (Fang-Yen et al., 2010), in which real *C. elegans* swims at wavelength $\lambda/L \approx 1.5$ and frequency $\approx 1.84 \text{ Hz}$, whereas our simulated worm swims at $\lambda/L = 1.5..1.7$ and frequency $1.75..1.79 \text{ Hz}$, which is very close to real values.

Suppl. Figure 3. Calculation of Viscosity in Sibernetic.

2.3. Calculation of Reynolds number in Sibernetic

The Reynolds number is defined as $Re = \rho vL/\mu$, where:

ρ is the density of the fluid (SI units: kg/m^3)	1000
v is the velocity of the fluid with respect to the object (m/s) (estimate for swimming <i>C. elegans</i> 's tail movement)	max $\approx 0.3 \text{ mm} / 0.25 \text{ s}$ $= 0.0012 \text{ m/s}$
L is a characteristic linear dimension (m), worm body diameter in this case	$60 \mu\text{m} = 6 \cdot 10^{-5} \text{ m}$

μ is the dynamic viscosity of the fluid (Pa·s or N·s/m ² or kg/m·s)	1.43 mPa·s \approx 0.0014 Pa·s
Re for marble with R=0.05 mm falling in liquid at $\mu = 1.43$ mPa·s Re for worm swimming at the same μ	0.27 \leq 0.05

Supplemental Table 2. Calculation of Reynolds number in Sibernetica

2.4. Physical constants & measurements

Name of the physical variable or constant	dimension	typical real value	actual value in simulation	comments
Constants				
'particle radius', r_0	m	n/a	$5.0 \cdot 10^{-6}$ (full-resol.) $1.1 \cdot 10^{-5}$ (half-resol.)	~ distance between two adjacent particles
particle mass	kg	n/a	$0.5 \cdot 10^{-13}$ (full-resol.) $2.0 \cdot 10^{-12}$ (half-resol.)	
worm length	mm	1.0 (Petzold et al., 2011) up to 1.3 (Mind of a Worm ⁵)	0.81...1.1	200· r_0 for full-resolution, 100· r_0 for half-resolution
worm diameter in its widest part	μ m	47.9 ± 0.8 (Maguire et al., 2011) up to 80 (Mind of a Worm ²)	61...67	12· r_0 , 6· r_0 , correspondingly
worm mass	kg	$2.1 \cdot 10^{-9}$	$2.04 \cdot 10^{-9}$	
liquid density, ρ_0	kg/m ³	1000	1000	water density
gravity acceleration	kg/(m·s ²)	-9.8	-9.8	
Measurements				
liquid viscosity	Pa·s	$0.89 \cdot 10^{-3}$ (water, 25° C) $1.0 \cdot 10^{-3}$ - typical most less viscous <i>C. elegans</i> swimming solution	$1.43 \cdot 10^{-3}$	Viscosity coefficient between agar and worm shell particles is 10 times less than visc. coeff. between all the rest combinations of particle pairs (2 agar particles, 2 worm body elastic particles, 2 liquid particles, liquid and any other particle, agar and any other particle etc.)
worm shell Young's modulus	Pa	1.3 ± 0.3 MPa (Bakholm et al., 2013) cuticle: 10–400 MPa, comparable to rubber (Zhen and Samuel, 2015) Cuticle: 380 MPa (Park et al., 2007) Bulk mechanical properties of <i>C. elegans</i> are independent of the cuticle (Gilpin et al., 2015). Worm as a whole: 140 ± 20 kPa, both for volumetric compression and expansion (Gilpin et al., 2015). Worm as a whole: $E = 3.77 \pm 0.62$ kPa (M. Backholm PhD thesis "Bio-mechanics of <i>C. elegans</i> ", 2015)	Young's modulus = stress/strain = $(F/A) \cdot L_0/(L_n - L_0)$. Using our values we get the following: $E \approx 41$ N/m ² or Pa for worm as a whole	Calculating the Young's modulus of the worm's body yields a value ranging from 110 kPa to 1.3 MPa, depending on whether the worm is modeled as a uniform cylinder or cylindrical shell (26). The large range of reported values highlights our poor understanding of the mechanical properties of <i>C. elegans</i> . There is a clear need for elucidating the role of the cuticle, as well as the interplay of internal and external pressure, in the mechanics of the whole worm.(Gilpin et al., 2015).

⁵ http://www.wormatlas.org/ver1/MoW_built0.92/description.html

Max <i>C. elegans</i> muscle cell force	N	An experimentally measured force exerted by the worm, not by just its single muscle, on the small object, has a value $\approx (8...18) \cdot 10^{-6}$ N (Johari et al., 2013). See Suppl. Methods 2.1 for more.	$2.7 \cdot 10^{-9}$ N (this value was taken from Fig 3B, right panel, cyan curve, at $L/L_0 = 1$, when muscle force exactly compensates external force)	in our current model cross-section of a single 'muscle cell' contains only a few...several 'muscle fibers'
Hydrostatic pressure inside the worm	Pa	2–30 kPa (Harris & Crofton, 1957) – for <i>A. suum</i> (large parasitic nematode), and for <i>C. elegans</i> there is no estimate yet.	estimate of extra pressure in the model, based on springs extension caused by, and corresponding Hookean force: 0.01 Pa	possibly such a big difference is due to the fact that we do not simulate the 'air', no atmospheric pressure, so no need to compensate high external pressure by high internal one.

Suppl. Table 3. Constants and measurements from the worm body model

2.5. Construction of realistic worm body prototype

We have constructed a proof of concept prototype of the worm body using the “materials” we have created above. A number of original subroutines were designed to build the worm body based on a set of parameters and set the initial configurations of particles, springs, muscles, membranes etc. They include the generation of worm body shell, represented by 2 layers of elastic matter particles (with a worm body width profile along head-to-tail direction highly similar to that of the real 1.1 mm long adult *C. elegans*), mapping of contractile muscle fibers onto it, and filling worm’s inner space with a liquid providing hydrostatic pressure. The outer surface of the worm body shell is completely covered by a set of membranes which prevents leakage of liquid from inside of the worm to the outside space.

The resolution of the model (number of particles representing the whole worm) can also be varied. The worm body model can be generated parametrically for a wide range of values, though the muscles still need manual mapping. Our current prototype is a compromise between high-detail and computational performance. It includes 10143 elastic matter particles and 11436 liquid particles composing worm body. The worm body is built as a composition of adjacent 1-particle-thick layers, stacked up along the direction from head to tail, each represented with a circle with radius equal to real worm’s radius at the same position along the body. Distance between particles within each circle and between adjacent circles is chosen to provide correct density value (1000 kg/m^3). Elastic matter connections and coverage by membranes is performed via a subroutine.

2.6. Cuticle as pressurized elastic shell

The real worm’s body is an elastic shell-type hydrostatic skeleton (Park et al., 2007) that contains an internal muscular system. Internal tissues are under hydrostatic pressure on the order of 2–30 kPa (Harris & Crofton, 1957). The multilayered cuticle has an elasticity, described by Young’s modulus, estimated to be within 1-1.6 MPa (Backholm et al., 2013; Gilpin et al., 2015).

The 3D worm body profile, as well as muscle positions and geometry, is designed to take into account the proportions of real *C. elegans* (Altun et al., 2015). Our *C. elegans* body model has a spindle-shaped form closely approximating that one of a real nematode.

The radius of the worm body along the length of the worm is known from microphotographs. The body of *C. elegans* is considered radially symmetrical. Typical values for a real adult worm are a length of 0.8...1.2 mm and a diameter of 60.80 μm in its widest part. The width profile along the length of the worm was estimated from microphotographs (Sulston & Horowitz 1977) and from the 3D model in the Virtual Worm Blender files (Grove & Sternberg, 2011) as shown in the OpenWorm Browser⁶.

The shell of the worm body is composed of nearly 100 or 200 rings (for the cases of low/high resolution) composing an elastic tube consisting of 2 layers of particles connected between each other within each layer and between them as well (Fig 1). The number of particles in each ring varies based on the actual radius at each considered position along the worm body.

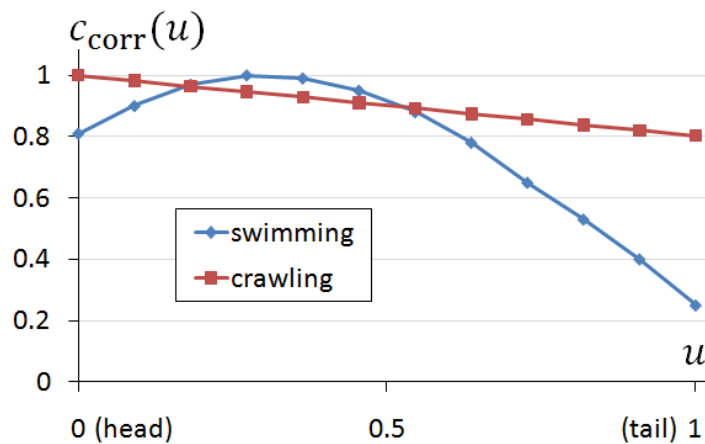
⁶ <http://browser.openworm.org>

The cavity inside the body shell is filled with liquid particles with a density a bit larger than ρ_0 to provide sufficient pressure to adequately keep it shaped cylindrically and prevent obvious deformations. We varied its amount to get maximally realistic properties and found that additional pressure of 0.01 Pa works well. While in the real worm it is estimated as 2-30 kPa. This may have to do with the fact that we are not simulating atmospheric pressure of air (approx. 100 kPa) back onto the worm's cuticle, therefore no force is resisting the internal pressure in our model as would exist in the real animal. We did not find any mention of this problem or its solution among previous approaches to *C. elegans* body modelling.

2.7. Activation of the muscles via computational interface

Each muscle contains some set of elastic connections which are able to contract depending on external signals and is able to be individually addressed and driven by signals from neurons or other source. Signals are represented as a sequence within the interval [0,1] (completely relaxed / completely activated). The signal is a float and it is read every simulation step. No explicit damping factor is used within individual activations, but as a result of the other relationships that exist in the system. The signal float value is multiplied by the maximal force. For a single muscle, it is done uniformly across all the contractile matter relationships across its length.

In order to produce behavioral output, a pattern of activation is applied to the muscle cells in different sequences. These activation patterns can be derived from the result of synaptic activation from a simulated nervous system, for example through Sibernetic-NEURON interface or via integration with c302⁷, a sub-platform of the OpenWorm project - a Python framework for simulation of multi-scale cell and network models of the *C. elegans* nervous system (Lung et al., 2017). However, in our tests for this article, scripted activation patterns have been used. These activation patterns create sinusoidal input to the muscle cells. In order to produce forward locomotion behaviors, the sinusoid presented to the DL and DR muscles is shifted by 90 degrees ($\pi/2$) compared to the sinusoid presented to the VL and VR muscles.



Suppl. Figure 4. Muscle force correction functions applied to force input to muscles in Sibernetic for different behavioral conditions. u refers to the position of a muscle along the length of the body, and $c_{\text{corr}}(u)$ is the value of the multiplicative factor to use with the muscle force strength.

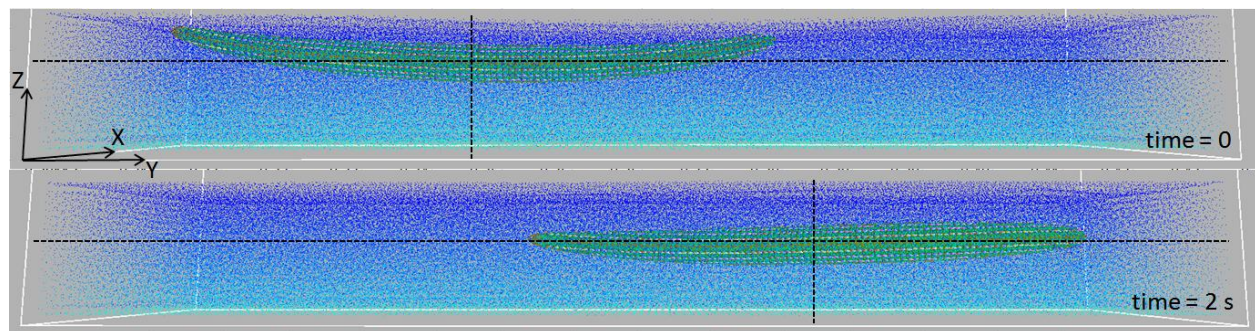
Across the muscles along the length of the worm's body, another function is multiplied with the strengths of the incoming signal, depending on the position along the body. Two different functions are used for shaping the activation signals to the muscles (Suppl. Fig. 4), one for swimming and one for crawling. They are necessary to provide realistic body shapes and movement. If all muscle cells were of equal length, these modifications would be unnecessary, but in the latest version of the body model they have shapes according to the photograph (Fig. 2), and thus muscles in the head and neck are much shorter than in the middle of the body.

2.8. Visualization of the worm body, muscles, and environment

In Sibernetic, which uses OpenGL for visualization, all particles are represented as points in 3D space and spring connections between elastic matter particles - with lines. Water particles are shown with blue (and sometimes are colored with blue-green-yellow gradient showing extra pressure), agar - with light-yellow or light-green-yellow. In case of crawling simulation "agar" particles, particles that come in contact with the worm body are colored differently than all the rest for easier worm trajectory tracking. Muscle fibers are usually displayed with colored lines, thicker for

⁷ <https://github.com/openworm/CElegansNeuroML/tree/master/CElegans/pythonScripts/c302>

currently active and thinner for inactive muscles. Four colors are used, a pair for each line of muscles in a quadrant, interchanging between neighbour muscles (see Fig. 2). Worm body color may differ; usually it is either green or gradient from light gray (head) to dark gray (tail). Membranes, when they are shown, are displayed with cyan triangles. The Simulation box is shown as well. It is possible to rotate, pan, and scale the scene via the mouse.



Suppl. Figure 5. A swimming worm swims through the middle of the liquid. Corresponding video is available⁸.

References

1. Park S.-J., Goodman M. B., & Pruitt B. L. (2007). Analysis of nematode mechanics by piezoresistive displacement clamp. *Proceedings of the National Academy of Sciences of the United States of America*, **104**(44), 17376–17381. (doi:10.1073/pnas.0702138104) <http://www.pnas.org/content/104/44/17376.full.pdf>
2. Harris B. Y. J. E., & Crofton H. D. (1957). Structure and Function in the Nematodes: Internal Pressure and Cuticular Structure in *Ascaris*. *Journal of Experimental Biology*, **34**, 116–130.
3. Altun Z.F., Herndon L.A., Wolkow C.A., Crocker C., Lints R. and Hall D. H. (ed.s) (2002-2018). *WormAtlas*. <http://www.wormatlas.org>
4. Williamson D. R. (2012). Modelling the locomotion nervous system in the nematode *C. elegans*: a developmental perspective. (doi=10.1.1.724.9775)
5. Lung D., Larson S., Palyanov A., Khayrulin S., Gleeson P., Zimmer M., Grosu R. and Hasani R.M.. A Simplified Cell Network for the Simulation of *C. elegans*' Forward Crawling // *Proc. 1st NIPS Workshop on Worm's Neural Information Processing (WNIP 2017)*, Long Beach, CA, USA., 2017
6. Cohen N., & Ranner T. (2017). A new computational method for a model of *C. elegans* biomechanics: Insights into elasticity and locomotion performance. Retrieved from <http://arxiv.org/abs/1702.04988>
7. Backholm M. (2015) Biomechanics of *C. elegans* as probed by micropipette deflection. PhD Thesis, McMaster University. <https://macsphere.mcmaster.ca/handle/11375/18317>
8. Niebur E., Erdös P. (1993) Theory of the locomotion of nematodes: control of the somatic motor neurons by interneurons. *Math Biosci.* **118**(1), 51-82.
9. Bryden J.A. and Cohen N. (2004) A simulation model of the locomotion controllers for the nematode *Caenorhabditis elegans*. In: Schaal S., Ijspeert A.J., Billard A., Vijayakumar S., Hallam J. and Meyer J-A., (eds.) *From Animals to Animats 8: Proceedings of the Eighth International Conference on the Simulation of Adaptive Behavior*. SAB'04, 13 - 17 July 2004, Los Angeles, CA, USA. MIT Press, Cambridge, Mass., pp. 183-192. ISBN 978-0-262-69341-7
10. Suzuki M., Tsuji T., Ohtake H. (2005) A model of motor control of the nematode *C. elegans* with neuronal circuits. *Artif Intell Med.* **35**(1-2), 75-86.
11. Karbowski J., Schindelman G., Cronin C.J., Seah A., Sternberg P.W. (2008) Systems level circuit model of *C. elegans* undulatory locomotion: mathematical modeling and molecular genetics. *J Comput Neurosci.* **24**(3), 253-76.
12. Rönkkö M., Wong G. (2008) Modeling the *C. elegans* nematode and its environment using a particle system. *J Theor Biol.* **253**(2), 316-22. doi: 10.1016/j.jtbi.2008.03.028.
13. Mailler R., Avery J., Graves J. & Willy N. (2010) A Biologically Accurate 3D Model of the Locomotion of *Caenorhabditis elegans*. *International Conference in Biosciences (BIOSCIENCESWORLD)*, 84-90.

⁸ https://www.youtube.com/watch?v=E_nggWLWAU

14. Palyanov A., Khayrulin S., Larson S.D., Dibert A. (2011) Towards a virtual *C. elegans*: A framework for simulation and visualization of the neuromuscular system in a 3D physical environment. *In Silico Biology* **11**, 137–147. <https://doi.org/10.3233/ISB-2012-0445>
15. Petzold B.C., Park S.J., Ponce P., Roozeboom C., Powell C., Goodman M.B., Pruitt B.L. (2011) *Caenorhabditis elegans* body mechanics are regulated by body wall muscle tone. *Biophys J.* **100(8)**, 1977-85.
16. Maguire SM, Clark CM, Nunnari J, Pirri JK, Alkema MJ. (2011) The *C. elegans* touch response facilitates escape from predacious fungi. *Curr Biol.* **21(15)**, 1326-30. (doi:10.1016/j.cub.2011.06.063)
17. Majmudar T., Keaveny E.E., Zhang J., Shelley M.J. (2012) Experiments and theory of undulatory locomotion in a simple structured medium. *J R Soc Interface*, **9(73)**, 1809-23. (doi:10.1098/rsif.2011.0856)
18. Johari S., Nock V., Alkaisy M.M., Wang W. (2013) On-chip analysis of *C. elegans* muscular forces and locomotion patterns in microstructured environments. *Lab on a Chip* **13(9)**, 1699-707. (doi: 10.1039/c3lc41403e)
19. Boyle J.H., Berri S., Cohen N. (2012) Gait Modulation in *C. elegans*: An Integrated Neuromechanical Model. *Front Comput Neurosci* **6**, 10. (doi: 10.3389/fncom.2012.00010)
20. VanBuren P., Guilford W.H., Kennedy G., Wu J., Warshaw D.M. (1995) Smooth muscle myosin: a high force-generating molecular motor, *Biophys J.* **68(4 Suppl)**, 256S-258S.
21. Grove C.A. & Sternberg P.W. (2011) The Virtual Worm: A Three-Dimensional Model of the Anatomy of *Caenorhabditis elegans* at Cellular Resolution. *In 18th International C. elegans meeting*. Retrieved from http://www.celegans.org/2011/pdf/abstracts_web.pdf